An Analysis of Chest X-ray by Laplacian Gaussian Filtering and Linear Opacity Judgment

Jin-Woo Kim, *Member, KIMICS*

Abstract— We investigated algorithm to detect and characterize interstitial lung abnormalities seen at chest radiographs. This method includes a process of 4 directional Laplaction-Gaussian filtering, and a process of linear opacity judgment. Two regions of interest (ROIs) were selected in each right lung of patients, and these ROIs were processed by our computer-analyzing system. For quantitative analysis of interstitial opacities, the radiographic index, which is the percentage of opacity areas in a ROI, was obtained and evaluated in the images. From or result, abnormal lungs were well differentiated from normal lungs. In our algorithm, the processing results were not only given as the numeric data named "radiographic index" but also confirmed with radiologists observation on CRT. The approach, by which the interstitial abnormalities themselves are extracted, is good enough because the results can be confirmed by the observations of radiologists. In conclusion, our system is useful for the detection and characterization of interstitial lung abnormalities.

Index Terms—Chest radiography, interstitial lung disease, Laplacian-Gaussian filter, image processing.

I. INTRODUCTION

Chest X-ray (radiography) remains the most common of imaging procedures for the diagnosis of interstitial lung disease and is used as an indicator of the necessity for further imaging examinations such as computed tomography [1]. However, evaluation of interstitial lung disease with chest radiographs is difficult. Various types of radiographic patterns are observed, and their changes are often subtle [2]. As well, the descriptions of radiographic findings by radiologists often lack objectivity and quantitative ness. If radiographic patterns of interstitial lung disease seen on chest radiographs can be quantitatively analyzed, this may improve the diagnostic accuracy.

The method of texture analysis has been used for quantitative analysis of interstitial lung abnormalities [3] ~[7]. In texture analysis of the lung region, the statistical approach is often used. Density variation and the optical Fourier spectrum are used as physical measures to classify lungs with interstitial disease. Quantification of the severity of pneumoconiosis also has been reported [8]~[12]. Other than pneumoconiosis, many reports have distinguished normal lungs from abnormal lungs with interstitial diseases by classification of the abnormality using texture analysis methods [3]~[7]. Katsuragawa et al [6, 7] developed a classification method for distinguishing between normal lungs and abnormal lungs with interstitial disease. They used a power spectrum analysis and a "visual system response" of human observers. They stated that the results corresponded to the visual characteristics that radiologists recognized.

Various types of interstitial radiographic patterns are observed in chest radiographs of patients with interstitial lung diseases. However, it is difficult to extract all of these patterns. Four basic roentgenographic patterns of interstitial diseases are presented: (1) reticular, (2) nodular, (3) reticulonodular, and (4) linear [13]. These patterns are correlated with their computed tomography findings. These four basic patterns were thought to consist of two patterns: one "nodular", and the other "linear". We roughly divided these radiographic patterns into two groups. One is a nodular opacity group and the other is a linear opacity group. A computerized analysis system that have developed can selectively extract the linear opacities processed by Laplacian-Gaussian filtering, binarization, and linear opacity judgment processing. In 100 patients with or without interstitial lung disease, we attempted to classify the radiographic patterns confirmed with high-resolution computed tomography (HRCT) using physical measurements obtained with our computerized analysis system.

II. METHODS

Chest radiographs were digitized and regions of interest (ROIs) were selected in the right upper and lower lung areas. To extract linear opacities selectively, four-directional Laplacian-Gaussian filtering, binarization, and linear opacity judgment processing were performed for each ROI. Finally, the radiographic index, which is a percentage of opacity areas in an ROI, was employed for evaluating the chest radiographs as a physical measure.

Manuscript received August 27, 2008; revised October 21, 2008.

Jin-Woo Kim is with the Department of Multimedia Communication Engineering, Kyungsung University, Busan, Korea. (Tel: +82-51-607-5153, Fax: +82-51-625-1402, Email: jinwoo@ks.ac.kr)

2.1 Digitization of the Chest radiograph

Conventional posteroanterior chest radiographs were digitized to 2,000×2,000 matrix with 1,024 gray levels by a laser scanner. We used a television-image processor and a personal computer or our image processing and analyzing system. Digitized images were recorded on a rewritable magneto-optical disk cartridge.

To select ROI for image processing and analyzing, the digitized image of the full chest radiograph was displayed on a cathode-ray tube (CRT). Two ROIs with a 296×296 matrix size (51.8mm×51.8mm) were selected manually in the right upper and the right lower lung area.

One ROI was selected at the level of upper pulmonary hilum in the right upper area and the other was selected above the diaphragm. To avoid hilar anatomical structures, both ROIs were selected apart from the hilum (Fig. 1). Had we selected a ROI in the left lower lung area, the ROI would overlap the cardiac opacity, which would cause poor image processing results. Therefore, we excluded this area from our evaluation. There was no such problem in the left upper lung zone. However, to evaluate our system by as many cases as possible and to avoid the bias based on the upper or lower lung area, we selected one ROI in the right upper lung area and one ROI in the right lower lung area of each case. In our study, no significant differences were found between the upper and lower ROIs.

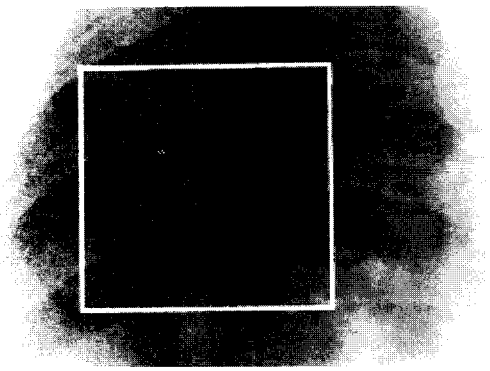

(a)normal lung

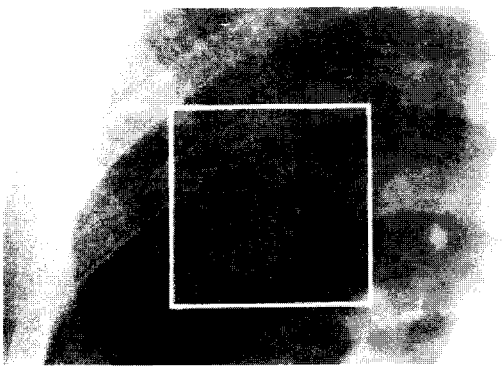

(b)abnormal lung

Fig.1 Chest radiographs of the right upper lung fields with ROIs.

2.2 Filtering by Laplacian-Gaussian Filter

To extract linear opacities in the selected ROI, we chose the Laplacian-Gaussian filter, which reflected the human visual perception [14]. This filter is given by the following:

$$\nabla^2 G(r) = \frac{2\sigma^2 - r^2}{2\pi\sigma^6} e^{\frac{r^2}{-2\sigma^2}}$$

Where $G(r)$ is the Gaussian distribution, r is the distance from the center of the filter and σ is the spatial spread parameter which corresponds to the standard deviation. This filter enhances elements of linear opacities in all directions. For this reason, we employed a new directional one-dimensional Laplction-Gaussian filter, which enhances specific directional elements. This filter is given by the following:

$$\nabla^2 G(X) = \frac{1}{\sqrt{2\pi\sigma^5}} (X^2 - \sigma^2) e^{\frac{X^2}{-2\sigma^2}}$$

Where X is the coordinate axis, perpendicular to a specific direction α_i. We changed i from 1 to 4 ($\alpha_1 = 0$, $\alpha_2 = \pi/4$, $\alpha_3 = \pi/2$, $\alpha_4 = 3\pi/4$) and obtained four processed images by using these four-directional Laplacian-Gaussian filter. The matrix size of this filter was 15×15 pixels. The width (2σ) of the center line of the filter just corresponds between the 1/e points of both sides of the maximum of the Gaussian function. In this study, we used the same Laplacian-Gaussian filter for all images.

In the images after processing, some peripheral part of the ROI became ineffective. Therefore, the following processing was carried out in the submatrix of 256×256.

The Laplcian-Gaussian filter has a band-pass characteristic with a peak at 1/ ($\sqrt{2\pi\sigma}$). The spatial frequency to be detected can be adjusted by selecting a suitable σ. This enables us to detect interstitial lung abnormalities well with the reduced noise. Moreover, this filter corresponds to a physiological model of human vision [14]. We set σ at 0.438mm in this system, because there was a relation of $w = 2\sigma$, where was a width of the line at the center of the filter. Because the suitable diameter of peripheral vessel opacities were thought to be approximately 0.5 to 1.0mm, the value of w should be set below this value.

Another advantage of the Laplacian-Gaussian filter was that correction of background trend caused by normal anatomical structures and the exposure condition was not required, because the background trend frequency was low enough compared with 1/($\sqrt{2\pi\sigma}$).

The original Laplacian-Gaussian filter does not have a specific directionality, but enhances in all directions in the same way. However, to extract linear elements of interstitial chest abnormalities, it was necessary for

the filter to have various directions on the image plane. Therefore, in our system, the filters with four directions (horizontal, vertical, and two diagonal directions $[\alpha_1 = 0, \alpha_2 = \pi/4, \alpha_3 = \pi/2, \alpha_4 = 3\pi/4]$ were used. This filter is not purely a Laplacian-Gaussian filter, since Laplacian means the sum of the second-order derivatives in horizontal and vertical axes, and our filter is only the second-order derivative in one direction. However, we called this filter a directional Laplaction-Gaussian filter or simply Laplacian-Gaussian filter. The Laplacian-Gaussian filter used in our system could extract an opacity in a specific direction. However, other elements as well as the linear opacities also were extracted. Moreover, the extracted linear opacity elements were not continuous, and the output image contained scattered pixel patterns. To extract the linear opacities well, further judgment processing of linear opacities was required. The first four-directional Laplacian-Gaussian filters extracted very shirt linear opacities or candidate pixels of linear opacities, and the second linear opacity judgment processing selected long opacities or true linear opacities from these pixels, Theoretically, similar results can be obtained if the linear opacities are extracted by using a large scale Laplacian-Gaussian filter with many directions.

2.3 Binarization

Binarization was performed for each image that had been processed with the four-directional Laplacian-Gaussian filter. Then, the summation image was obtained by adding the four binary images. We have no conclusive method to select a suitable threshold of binarization that only can extract interstitial lung opacities. One reason is that various kinds of radiographic patterns are included and their changes are often subtle [2]. Another reason is that radiologists descriptions of radiographic patterns often lack objectivity and quantitativeness. We selected five candidates of the threshold for 20 cases, based on the observations of the radiologists, Next, we selected one threshold for this system based on the results of the preliminary study. This same threshold was applied to all images.

2.4 Linear Opacity Judgment Processing

To extract linear opacities selectively, a method of linear opacity judgment processing was carried out for the four binary filtered images (Fig. 2). In this method, we choose a search line method which detects linear opacity elements.

The search line method used in the liner opacity judgment processing is a method of detecting straight line segments directly on the image plane. We separately applied this method to each of the binary images obtained by four-directional Laplacian-Gaussian filtering, Finally, the summation image was obtained by adding the four linear opacity judgment processing images. This was necessary because, if the judgment processing was conducted after summing the four-directional Laplacian-Gaussian filtering output, specification of linear opacity direction became difficult. This might result in mistakes in linear opacity judgment.

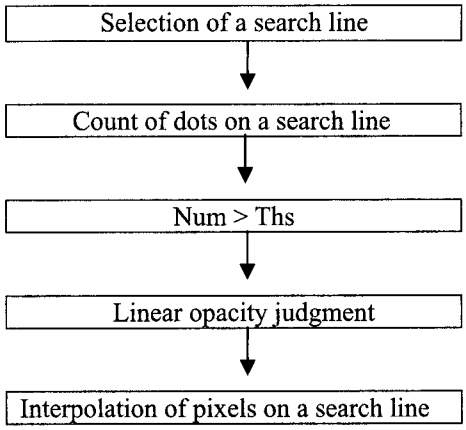

Fig. 3 Scheme for linear opacity judgment processing (Num is the total number of pixels on a search line and Ths is the threshold. If N>Ts, then pixels on a search line ate judged as those of a linear opacity.)

First, the search line of θ and Ls is selected on all pixels within ROI, where θ is a certain direction and Ls is the length of the search line. Next, the number (Num) of pixels on the search line is counted. If N is greater than a threshold (Ths), these pixels are determined as elements of the linear opacity. Pixels between the pixels that are determined as elements of the linear opacity are interpolated. For each pixel in the image, this process is repeated for θ at every $\pi/36$ within the range of $\alpha_i - \pi/4$ to $\alpha_i + \pi/4$.

In each case of i ($\alpha_1 = 0, \alpha_2 = \pi/4, \alpha_3 = \pi/2, \alpha_4 = 3\pi/4$), the processed image of linear opacity judgment processing is obtained. Finally, the summation image is obtained by adding the four processed images of linear opacity judgment processing. In this study, we decided that Ls was 30 pixels and Ts was 24 pixels. These values were determined by results from a preliminary study using several cases.

linear opacity judgment processed images in Fig. 3, obtained from a normal case and an abnormal case correspond, respectively, to the normal case and the abnormal case in Fig. 1. Figures 3a and 3b are the processed images of the abnormal case. Figures 3c and 3d are the processed images of the abnormal case. Figures 3a and 3c are the summation images of four-directional Laplacian-Gaussian filtering and binarization. Figures 3b and 3d are the summation images obtained by adding the four processed images of linear opacity judgment processing.

2.5 Calculation of Radiographic Index

To evaluate interstitial lung opacities, we employed a

radiographic index as a physical measure. The radiographic index is the percent area of extracted opacities to the ROI, a simple way to evaluate our method, which correlated well with the extent of interstitial lung abnormalities. Radiographic index d was obtained from the summation image of the four images processed with Laplacian-Gaussian filtering and binarization, and from that of the four processed images of linear opacity judgment. The significant difference between the values of these radiographic indices was examined by the unpaired Student's t-test [15].

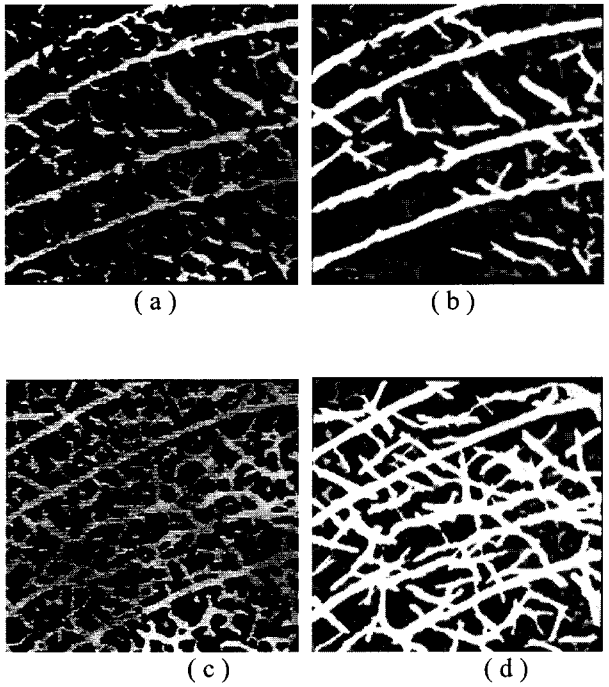

Fig.3 Outputs of 4-directional Laplacian-Gaussian filtering and liner opacity judgment processing in the selected ROIs (256X256 matrix size) (a) Image of the ROI for a normal lung obtained from the summation of 4-directional Laplacian-Gaussian filtering and binarization, (b)Image of the ROI for a normal lung obtained from the summation of 4-directional linear opacity judgment processing, (c)Image of the ROI for an abnormal lung obtained from the summation of 4-directional Laplacian-Gaussian filtering and binarization, (d)Image of the ROI for an abnormal lung obtained from summation of 4-directional linear opacity judgment processing.

2.6 Classification of Interstitial Lung Opacities in the High-Resolution Computed Tomography Images

To evaluate our system, interstitial lung opacities found on HRCT were classified into two patterns: (1) honeycombing group, and (2) others group. Honeycomb opacities were found to be dominant on HRCT. This group often represents typical linear opacities in chest radiographs. Others group abnormal opacities were found on HRCT, but these were excluded from honeycombing group. Others group included pulmonary abnormalities such as small nodular opacities and ground-glass opacities. Each ROI selected in the chest radiographs was classified according to its corresponding HRCT findings into two groups (Honeycombing Group, n=21: Others Group, n=79).

III. EXPERIMETAL RESULTS

Abnormal lungs were well differentiated from normal lungs by the radiographic indices obtained from the images filtered by four-directional Laplacian-Gaussian filters and from those processed by linear opacity judgment. Table 1 shows significant differences in each of the radiographic indices were observed between the normal group and the abnormal group ($P < .001$).

Table.1 Radiographic indices of the normal and abnormal lungs.

	Normal lungs (n=50)	Abnormal lungs (n=50)
dbin	24.1 ± 5.8	36.7 ± 5.0
dlin	15.1 ± 6.0	27.0 ± 6.4

Note: Each value is mean $\pm$ one standard deviation.
dbin : processed by 4-directional Laplacian-Gaussian filtering.
dlin : processed by linear shadow judgment.

Table 2 shows that significant differences were observed in **dlin** between honeycombing group and others group ($P < .05$), while no significant differences were observed in **dlin** between honeycombing group and others group.

Table. 2 Comparison of radiographic indices and image feature of High-resolution computed tomography.

	Honeycombing (n=21)	Other (n=79)
dbin	24.1 ± 2.7	38.8 ± 5.2
dlin	33.0 ± 3.4	29.8 ± 6.8

IV. CONCLUSIONS

We used two kinds of "radiographic indices" as physical measures, one obtained from the images only processed by four-directional Laplacian-Gaussian filtering and the other obtained from the images

processed by linear opacity judgment processing. Our computerized analysis system could detect and classify interstitial lung abnormalities using digitized chest radiographs that were confirmed with HRCT. The results of evaluating whether this system was able to detect and to classify interstitial lung abnormalities from the digitized chest radiographs were as follows.

Both **dbin** and **dlin** made it possible to distinguish between normal cases and abnormal cases. Therefore, this system was able to detect interstitial lung abnormalities seen on chest radiographs.

Only in **dlin**, significant differences were observed between honeycombing group and other group, indicating that more linear opacities were extracted with linear opacity judgment processing than only with the corresponding binary images of the Laplacian-Gaussian filtering.

These results indicate that this system is useful for the detection and characterization of interstitial lung abnormalities.

REFERENCES

[1] F.A.Mettler, "Diagnostic radiology: usage and trends in the United States," Radiology, 162, pp. 263-266, 1987

[2] G.P.Genereux, "Pattern recognition in diffuse lung disease," Med Radiogr Photogr, 61, pp. 2-31, 1985

[3] R.N.Sutton, and E.L.Hall, "Texture measures for automatic classification of pulmonary disease," IEEE Trans Comput, 21, pp. 667-676, 1972

[4] J.Revesz, and H.L.Kundel, "Feasibility of classifying disseminated diseases based on their Fourier spectra," Invest Radiol, 8, pp.345-349, 1973

[5] R.J.Tully, et al, "Toward computer analysis of pulmonary infiltration," Invest Radiol, 13, pp. 298-305, 1978

[6] S.Katsuragawa, et al, "Image feature analysis and computer-aided diagnosis in digital radiography: detection and characterization of interstitial lung disease in digital chest radiographs," Med Phys, 15, pp. 311-319, 1988

[7] S.Katsuragawa, et al, "Image feature analysis and computer-aided diagnosis in digital radiography: classification of normal and abnormal lungs with interstitial disease in chest images," Med Phys, 16, pp. 38-44, 1989

[8] R.P.kruger, er al, "Computer diagnosis of pneumoconiosis," IEEE Trans Syst Man Cybern, 4, pp. 40-49, 1974

[9] A.F.Tumer, et al, "Automated computer screening of chest radiographs for pneumoconiosis," Invest Radiol, 11, pp. 258-266, 1976

[10] J.R.Jagoe, and K.A.Paton, "Reading chest radiographs for pneumoconiosis by computer," Br J Ind Med, 32, pp. 267-272, 1975

[11] J.R.Jagoe, "Gradient pattern coding: an application to measurement of pneumoconiosis in chest x-rays," Comput Biomed Res, 12, pp.1-15, 1979

[12] S.Katsuragawa, et. al, "Quantitative computer- aided analysis of lung texture in chest radiographs," Radiographics, 10, pp.257-269,1990

[13] R.G.Fraser, et al, "Roentgenologic signs in the diagnosis of chest disease," In: Diagnosis of diseases of the chest. Philadelphia, PA: W.B. Saunders, pp. 458-687, 1988

[14] D.Marr, E.Hilderth, "Theory of edge detection," Proc Royal Soc of London, B, 207, pp. 187-217, 1980

[15] D.Colquhoun, "Lectures on biostatistics," London, England: Oxford University Press, 1971

Jin-Woo Kim

He received the B.S degree in Electrical Engineering from Myongji University in 1992 and the M.S and Ph.D. degrees in Electronic Engineering and System design Engineering from Fukui University, Fukui, Japan, in 1996 and 1999, respectively. From 1998 to 1999, he was a researcher at Fukui University, Fukui, Japan. From 2000 to 2003, he was a contract Professor in the Department of Information communication and Computer Engineering at Hanbat National University, Daejeon, Korea. Since 2003 he has been with the Department of Multimedia communication Engineering at Kyungsung University, Busan, Korea, where he is currently an assistant professor. He is now a visiting researcher in the Department of Bioengineering at Tokyo University, Japan. His current research interests include image processing, pattern recognition, and medical imaging technology.